Organic & Biomolecular Chemistry

PAPER

View Article Online
View Journal | View Issue

Cite this: *Org. Biomol. Chem.*, 2014, **12**, 2559

Molecular binding behavior of a bispyridinium-containing bis(β-cyclodextrin) and its corresponding [2]rotaxane towards bile salts†

Ying-Ming Zhang, Ze Wang, Yong Chen, Hong-Zhong Chen, Fei Ding and Yu Liu*

Received 22nd October 2013,
Accepted 27th January 2014

DOI: 10.1039/c3ob42103a

www.rsc.org/obc

Bispyridinium-bridged bis(β-cyclodextrin) (**1**) and its corresponding [2]rotaxane (**2**) were synthesized by a 'click' reaction, in which two different types of macrocycles, cucurbit[7]uril and β-cyclodextrin, are employed as the wheel component and bulky stopper, respectively. Moreover, the molecular binding behaviors of hosts **1** and **2** with four bile salts, namely, the sodium salts of cholic acid (CA), deoxycholic acid (DCA), glycocholic acid (GCA), and taurocholic acid (TCA), were comparatively investigated by ^{1}H NMR spectroscopy and isothermal titration calorimetry experiments. The spectroscopic and microcalorimetric results can jointly demonstrate a cucurbituril-mediated binding process; that is, the introduction of cucurbit[7]uril has a pronounced impact on the electrostatic attraction and hydrogen-bonding interaction between the bispyridinium spacer in the host molecules and the hydrophilic terminal group in the guest molecules, ultimately giving a significant change in the thermodynamic origins of these supramolecular complexes.

Introduction

Researchers have reached a general consensus that synthetic receptor molecules can undoubtedly provide a completely new dimension for drug discovery and may bring a novel therapeutic approach in clinic application.[1] Within this regard, the complexation of functional substrates with native and modified cyclodextrins (CDs) can not only orchestrate the elaborate topological architectures,[2] but also endow these supramolecular complexes with enhanced biocompatibility and bioactivity.[3] In particular, among the most commonly employed bioactive substrates, it has been proven that bile salts and their steroidal analogues can be readily encapsulated in the CD cavity, mainly due to the greater size-fit efficiency between CD and the bulky aliphatic head group.[4] For instance, BRIDION® (Sugammadex), an extended γ-CD derivative with eight carboxylic groups at its primary face, can be clinically used as a reversal agent to specifically inhibit residual neuromuscular blockade in postoperative recovery, because the binding affinity between this synthetic receptor and the steroidal neuromuscular blocking agent rocuronium bromide can reach up to 10^7 M^{-1} order of magnitude under physiological conditions.[5]

Recently, we reported the inclusion mode and molecular selectivity of modified β-CDs with amino acids as chiral side arms, revealing that the introduction of chiral chromophoric substituents onto the rim of the CD cavity is an effective way to increase the binding ability and selectivity toward bile salts.[6] Additionally, through scrutinizing guest molecular structures, it can be found that the hydrophilic and negatively charged tail of bile salts, which play an important part in performing its biological functions in living processes, can also provide an active binding site to form an electrostatic complex with the oppositely charged counterparts. This structural feature inspires us to hypothesize that a better affinity may be achieved through the incorporation of bile salts with some appropriate hosts possessing positively charged substituents, because the electrostatic attraction is unanimously considered as the primary driving force to further stimulate other noncovalent interactions in the formation of functionalized supramolecular assemblies.[7]

To verify this hypothesis, the bispyridinium-bridged bis(β-CD) (**1**) and its corresponding [2]rotaxane (**2**) bearing a bispyridinium spacer were synthesized to comparatively investigate the multiple noncovalent interactions with four steroid guests, *i.e.*, the sodium salts of cholic acid (CA), deoxycholic acid (DCA), glycocholic acid (GCA), and taurocholic acid (TCA), with the aim of demonstrating the cooperativity of two

Department of Chemistry, State Key Laboratory of Elemento-Organic Chemistry, Nankai University, Collaborative Innovation Center of Chemical Science and Engineering, Tianjin 300071, P. R. China. E-mail: yuliu@nankai.edu.cn

† Electronic supplementary information (ESI) available: characterization data of hosts **1** and **2**, cyclic voltammograms, Job's plots, as well as 2D NMR spectra of the supramolecular complexes. See DOI: 10.1039/c3ob42103a

adjacent CD cavities and the additional contribution of an electrostatic attraction arising from the bispyridinium linkers. Despite the fact that the thermodynamic data of various supramolecular complexes have been known and collected for several decades,[8] controlled molecular binding behaviours involving CD-based (poly)rotaxane structures were rarely explored[9] and thus should deserve our special concern. Therefore, the present work will allow us to fully understand the structure–activity relationship and molecular recognition mechanism in this interesting, but less known, area of supramolecular chemistry.

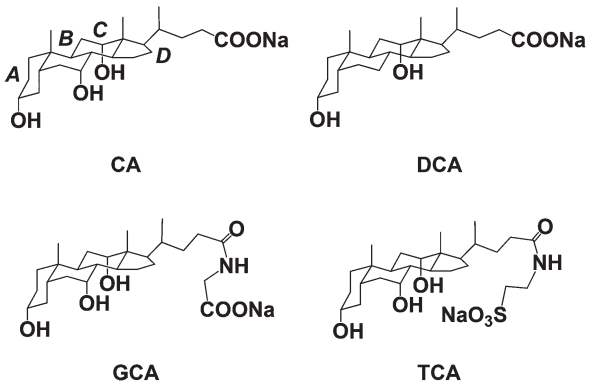

Chart 1 Molecular structures of employed guest molecules.

Results and discussion

Synthesis

The synthetic routes to bispyridinium-bridged bis(β-CD) (**1**) and its corresponding [2]rotaxane (**2**) are described in Scheme 1. Di(butynyl) bispyridinium salt (**3**) was prepared from 4,4′-bipyridine and 4-bromo-1-butyne in DMF. Then, mono-6-deoxyl-6-azido-β-CD (**4**)[10] was reacted with the intermediate **3** and [2]pseudorotaxane **3**⊂CB[7] through a 'click' reaction to afford the triazole-linked hosts **1** and **2** in a satisfactory yield. As shown in Fig. S7 and S8,† the chemical shifts at 4.15, 5.42, and 5.62 ppm in ^{1}H NMR spectrum, as well as 52.7, 71.2, and 156.1 ppm in ^{13}C NMR spectrum, jointly demonstrate the successful threading of CB[7] onto the bispyridinium axle in [2]rotaxane **2**. The compositions of all products were comprehensively verified by NMR spectroscopy and high-resolution MALDI-MS (Fig. S1–S9 in the ESI†). The molecular structures of guests are shown in Chart 1.

^{1}H NMR titration and electrochemical study

It is well-known that the complexation of CB[7] with various substrates, such as positively charged aromatic conjugates and metal complexes, is always accompanied by a remarkable chemical shift change ($\Delta\delta$).[11] First of all, the inclusion complexation behaviors of bispyridinium axle **3** with CB[7] were primarily studied by ^{1}H NMR titrations. As shown in Fig. 1, the proton signals of H_a, H_b, and H_c in **3** undergo an obvious complex-induced upfield shift upon incremental addition of CB[7] ($\Delta\delta_{a,3\subset CB[7]} = -0.32$ ppm, $\Delta\delta_{b,3\subset CB[7]} = -0.37$ ppm, and

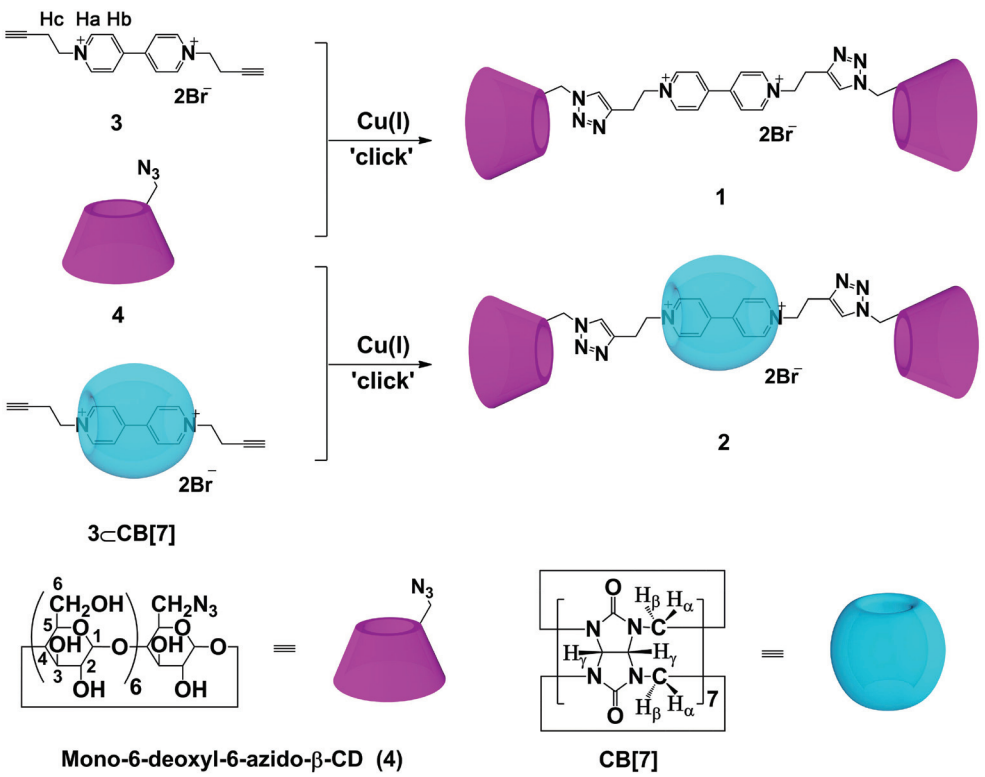

Scheme 1 Synthesis and proton designations of bispyridinium-containing bis(β-CD) (**1**) and [2]rotaxane (**2**).

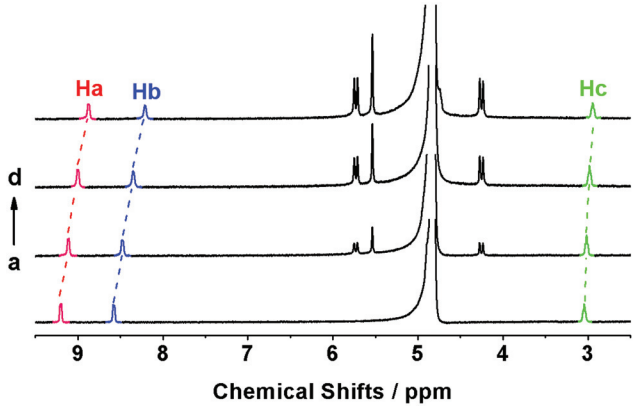

Fig. 1 ^{1}H NMR spectral changes of **3** upon addition of CB[7] in D_2O at 25 °C ([**3**] = 1.0 × 10^{-3} M, [CB[7]] = 0, 0.3, 0.6, and 1.0 × 10^{-3} M, from a to d).

$\Delta\delta_{a,3\subset CB[7]}$ = −0.10 ppm), indicating that the bispyridinium moiety of **3** is symmetrically located in the cavity of CB[7]. Moreover, as shown in Fig. S10,† the formation of [2]pseudorotaxane **3**⊂CB[7] was further confirmed by ESI-MS, in which the peak at *m*/*z* 712.7 could be clearly assigned to $\{\mathbf{3} + CB[7] - 2Br\}^{+\bullet}$.

Subsequently, Job's plots were performed to explore the complex stoichiometry by ^{1}H NMR titration, in which the total molar concentrations of host and guest components are fixed, and the chemical shifts of guest protons are accordingly changed upon the host–guest molecular ratios.[12] In our cases, an inflexion point at a molar fraction of 0.5 was observed in all the examined complexes, corresponding to 1 : 1 host–guest stoichiometry. Typical Job's plots for complexes GCA⊂**1** and CA⊂**2** are illustrated in Fig. 2, and very similar curves were also obtained in the complexation of **1** and **2** with other guest molecules (Fig. S11 in the ESI†). In addition, the electrochemical properties of **1** and **2** were investigated by cyclic voltammetry. As compared to the bridged CD dimers **1**, the first and second reduction peaks of the bispyridinium moiety in [2]rotaxane **2** show an obvious negative shift in the presence of CB[7], suggesting that the bispyridinium unit in **2** is included and stabilized by CB[7] (Fig. S12 in the ESI†).

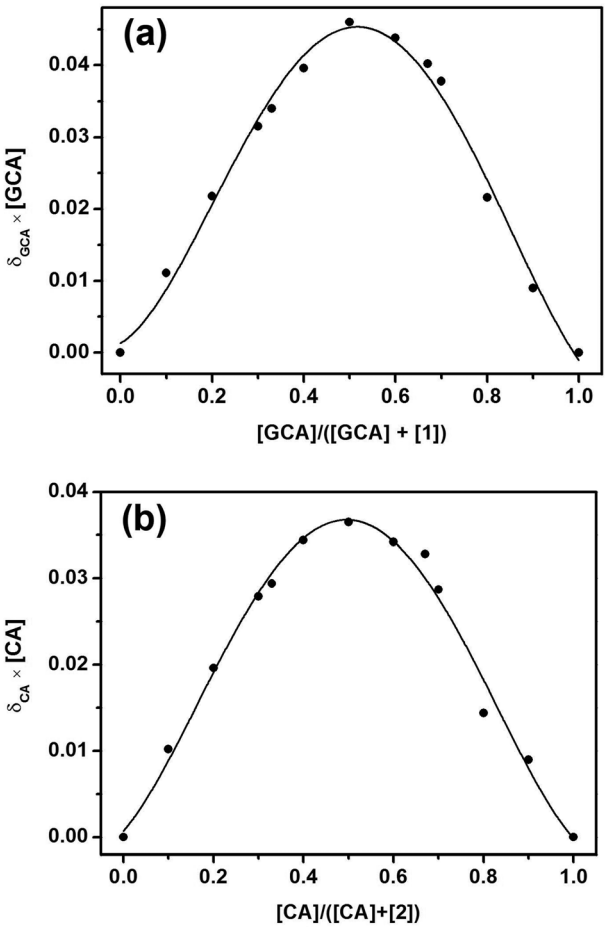

Fig. 2 Typical Job's plots of complexes (a) GCA⊂**1** and (b) CA⊂**2** in D_2O at 25 °C ([**1**] + [GCA] = [**2**] + [CA] = 1.0 × 10^{-3} M).

Binding mode

Two-dimensional NMR spectroscopy is a significantly informative method to obtain the binding geometries about the spatial arrangements of pendant substituent or included guest by analyzing the peak position and signal intensity of the nuclear Overhauser enhancement (NOE) cross-correlations.[13] Therefore, rotating-frame Overhauser effect (ROESY) and nuclear Overhauser enhancement spectroscopy (NOESY) experiments were further performed to obtain the conformation of hosts and host–guest complexes in aqueous solution. As shown in Fig. S13,† no obvious NOE correlation could be found between the bispyridinium linker and CD's interior protons, because the hydrophilic spacer with positive charges in **1** can seriously inhibit the formation of a self-inclusion complex. In contrast, the NOE cross-peaks between the triazole rings and CD's H5/H6 protons definitely confirm that the triazole groups of **2** are accommodated in the hydrophobic cavity of β-CD from the narrow opening of the cavity (peaks A and A′ in Fig. 3). Moreover, the correlations between the exterior $H_{\alpha,\gamma}$ protons of CB[7] and CD's H5/H6 protons were also observed, corroborating that CB[7] is symmetrically located in the vicinity of CD's primary face (peaks B in Fig. 3). Therefore, we can deduce that the molecular conformational changes for hosts **1** and **2** are contributing to the shielding effect of CB[7], by which the charge density of bispyridinium moiety can be reduced to a great extent.

As seen in Fig. 4, peak C is assigned to the NOE correlations between the G18 protons of CA and β-CD's H5 protons, peak D is assigned to the NOE correlations between the G21 protons of CA and β-CD's H3/H5 protons, and no correlation could be observed with the G19 protons of CA. Based on this information, we can infer that the D ring and the hydrophobic tail of CA enter the β-CD cavity from the secondary face to facilitate mutual electrostatic attraction with the bispyridinium center, leaving the A ring of CA outside the β-CD cavity. More interestingly, there is an obvious correlation of β-CD's exterior H2/4

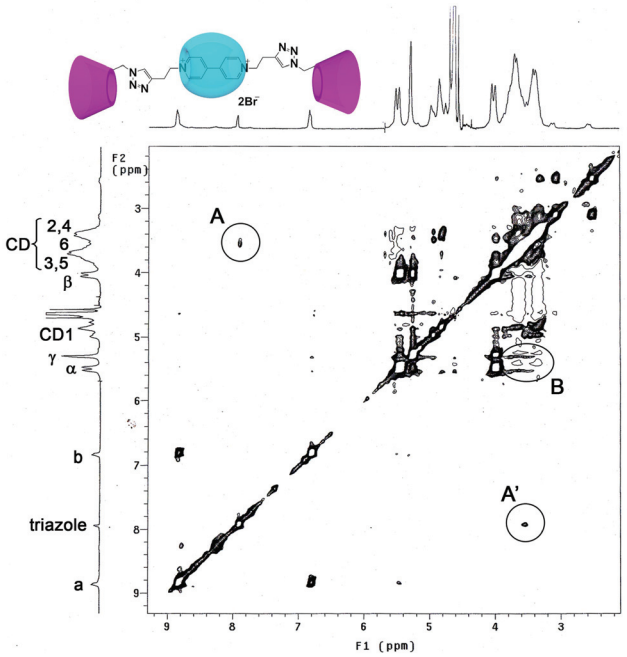

Fig. 3 ^{1}H NOESY spectrum of host **2** after a mixing time of 0.200 s ([**2**] = 2.2 × 10^{-3} M, 300 MHz, D_2O, 25 °C).

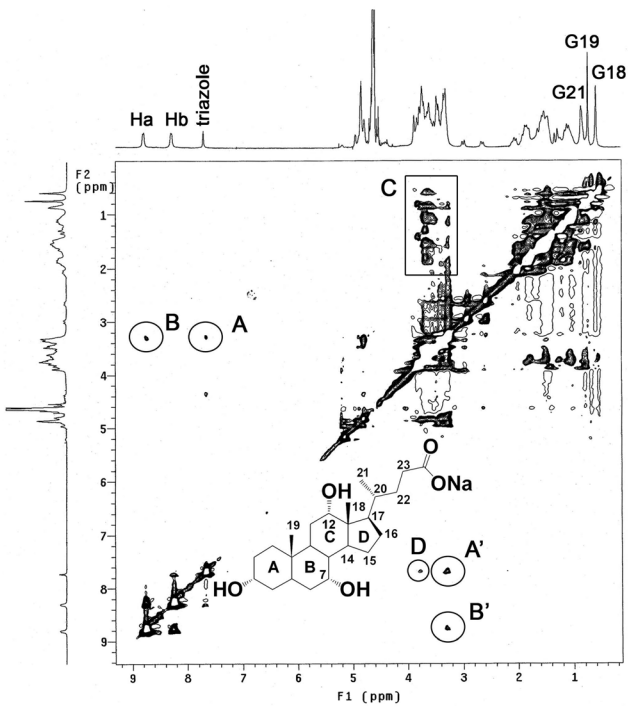

Fig. 4 ^{1}H NOESY spectrum of complex CA⊂**1** after a mixing time of 0.210 s ([**1**] = 2.2 × 10^{-3} M and [CA] = 5.0 × 10^{-3} M, 300 MHz, D_2O, 25 °C).

protons with the bispyridinium axle and triazole units (peaks A, A′, B, and B′), and peak D shows the NOE correlation between the triazole unit and β-CD's interior H3/5 protons. Considering the length and rigidity of the spacer, a direct and simultaneous inclusion of the triazole moiety with the CD's primary and secondary face can be reasonably excluded from the viewpoint of steric hindrance. Recently, the tumbling behavior of CD derivatives has stimulated increasing attention, in which one of the CD glucopyranose units can undergo 360° rotation around α-(1,4)-glucosidic bonds and thus make a pronounced effect on the intra/intermolecular binding mode of host compounds.[14] For example, the triazole-containing bridged bis(β-CD)s can exhibit a slow exchange equilibrium and adopt two different conformations in water.[14c] Of which, the minor supramolecular species are characterized by two unoccupied CD cavities, whereas the major ones are identified as an unsymmetrical structure with free and self-included CD cavities. Therefore, combining these fascinating results with the aforementioned complex stoichiometry and 2D NMR experiments, we can infer that one CD cavity in host **1** is occupied by CA guest, and the other one is filled with the triazole spacer originating from the tumbling of the glucopyranose unit (Fig. 5a and 5b).

Comparatively, the 2D NMR spectrum of CA⊂**2** complex in Fig. S14† seems a little more intricate, mainly due to the NOE correlations between the exterior protons of CB[7] and β-CD (peaks A and A′), as well as the intramolecular contacts in the bispyridinium axle of **2** (peaks B and B′). It should be noted that, as compared to the NOE cross-peak intensity in host **2** (peaks B in Fig. 2), the one in complex CA⊂**2** is remarkably stronger and more symmetrical (peaks A and A′ in Fig. S14†), implying that a conformational conversion may occur upon host–guest complexation to bring CB[7] and β-CD in close contact (Fig. 5c and 5d). Similarly, the peaks C contain the NOE correlations of G18 and G21 protons with the interior H3/H5 CD protons, here again indicating the encapsulation of the D ring and carboxylic tail inside the CD cavity. In contrast, some intense correlations were observed in the H5/H6 CD protons with bispyridinium and triazole units (peaks D and E). These cross-peaks jointly indicate that the positively charged axle is shallowly around the narrow opening of **2**. In addition, peaks F further indicate that the triazole moieties in host **2** still maintain two different conformations with the CD cavity. In our case, it is not surprising to conclude that one of CD cavities is still standing idle in the complexes of CA⊂**1** and CA⊂**2**, as the two CA guests cannot be concurrently accommodated in one host molecule because of the self-inclusion of triazole units and the serious bulkiness of CB[7]. Furthermore, 2D NMR experiments of **1** and **2** with DCA, GCA, and TCA were carried out to comprehensively study the binding behaviors in these host–guest complexes. Similar to complexes CA⊂**1** and CA⊂**2**, the NOE cross-peaks of the bispyridinium and triazole units with the cavity of β-CD were also found in the presence of other bile salt guests (peaks A–A′ and B–B′ in Fig. S15–S17,† and peaks B–D in Fig. S18–S20 in the ESI†). These phenomena demonstrate that the introduction of negatively charged bile salts may induce the tumbling of the glucopyranose unit in the inversion process.

The different binding manners of free dimers and their supramolecular complexes may be contributed to by the

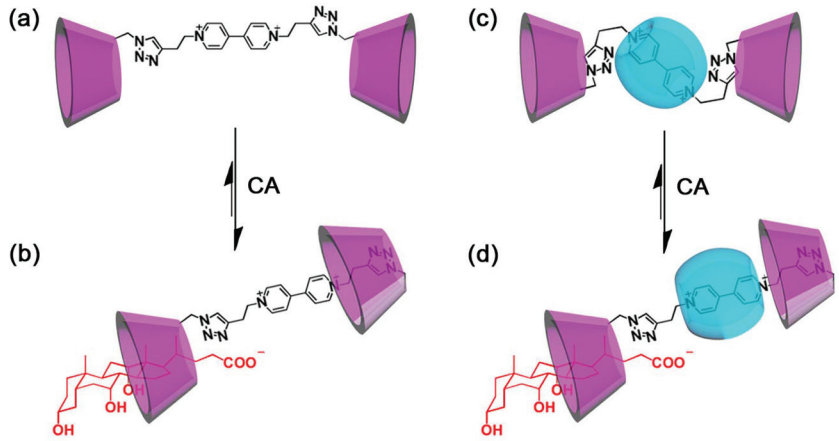

Fig. 5 Plausible molecular binding modes of (a) **1**, (b) complex CA⊂**1**, (c) **2**, and (d) complex CA⊂**2**.

significant change in charge density of the bispyridinium linker. Compared to compound **1**, the introduction of CB[7] can greatly decrease the charge density of the bispyridinium moiety through ion–dipole interaction, and then result in the self-included intramolecular complex between the triazole unit and CD cavity. Moreover, the inclusion complexation of bile salts possessing a negatively charged terminal group can not only occupy one CD cavity to release the triazole moiety, but also have a significant impact on the charge density of the bispyridinium linker to trigger the tumbling process of the neighboring CD unit. For example, the possible binding modes of CA with hosts **1** and **2** are shown in Fig. 5.

Microcalorimetric titration and thermodynamics

The thermodynamic origins of the supramolecular complexation of **1** and **2** with four steroids were quantitatively investigated by means of isothermal titration calorimetry (ITC) in aqueous buffer solution (Fig. 6 and 7). For a comparative purpose, those thermodynamic parameters for native β-CD with guests in the reported literature are also listed in Table 1.[15] As judged from Table 1, the thermodynamic stability constants (K_S) for dimeric hosts **1** and **2** with four guests are in the range from 10^3 to 10^4 M^{-1} orders of magnitude, and concretely, the K_S values for complexation of hosts **1** and **2** with all the guests decrease in the following sequence (Fig. 8):

$$\mathbf{1}: \text{CA} > \text{DCA} > \text{GCA} > \text{TCA}$$

$$\mathbf{2}: \text{TCA} > \text{GCA} \sim \text{DCA} > \text{CA}$$

It can be found that the K_S values in the dimeric hosts **1** and **2** are mostly larger than the ones in native β-CD, except that there is a reverse phenomenon in CA⊂**2** and DCA⊂**2** with a relatively lower stability. Generally, the higher stability in the dimeric hosts **1** and **2** is ascribable to the bispyridinium spacer and two hydrophobic cavities in close proximity, by which the supramolecular positive cooperativity can take place in the molecular binding process. Moreover, it is interesting to note that the gap of host selectivity is gradually reduced in

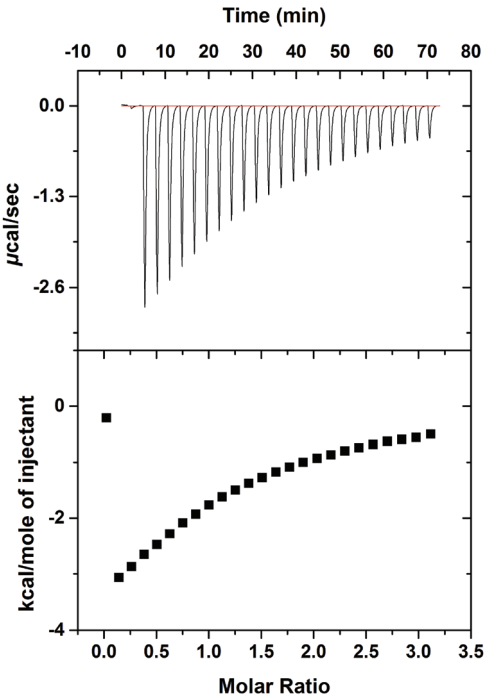

Fig. 6 Raw data and apparent reaction heat in calorimetric titrations for 25 sequential injections (10 μL per injection) of host **2** solution (3.33 × 10^{-3} M) injecting into CA solution (1.97 × 10^{-4} M) in phosphate buffer solution (0.1 M, pH 7.2) at 25 °C.

an order of CA > DCA > GCA > TCA ($K_S^{CA\subset 1}/K_S^{CA\subset 2} = 3.8$, $K_S^{DCA\subset 1}/K_S^{DCA\subset 2} = 2.9$, $K_S^{GCA\subset 1}/K_S^{GCA\subset 2} = 2.0$, and $K_S^{TCA\subset 1}/K_S^{TCA\subset 2} = 1.1$). Considering that all the employed bile salts are composed of similar steroidal skeletons, the large disparities of binding stability mainly originates from the hydrophilic tail of the guests. As the length of the hydrophilic tail increases, it is found that the K_S values of host **2** accordingly increase, with a maximum in the complex of TCA⊂**2**. In addition, it can also be seen that the contribution of CB[7] could be negligibly ignored in the case of TCA by elongating the length of the hydrophilic tail and the charge distances

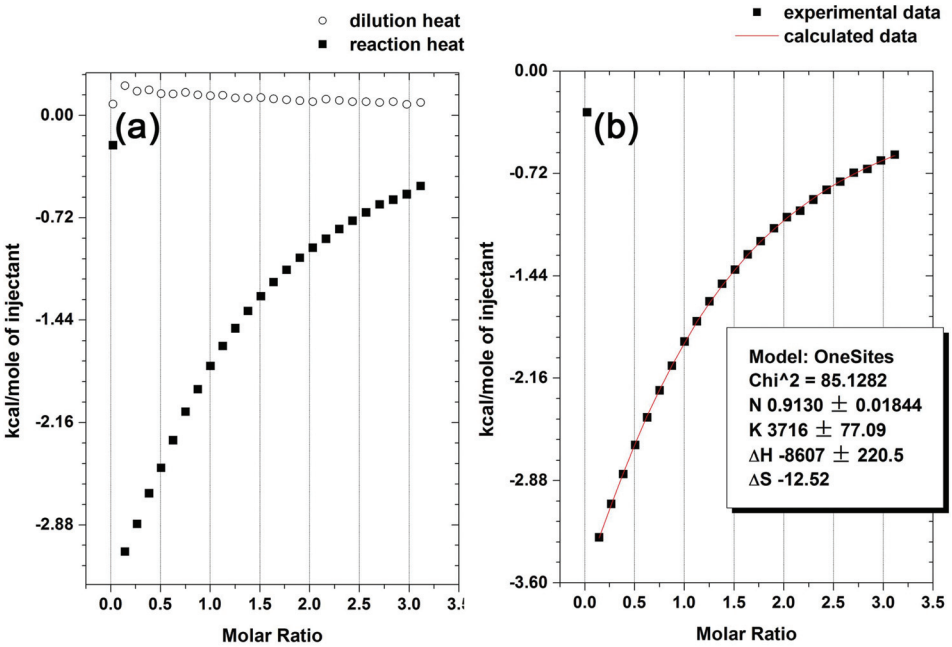

Fig. 7 (a) Heat effects of the dilution and of the complexation reaction; (b) typical ITC fitting curves of CA⊂**2** in phosphate buffer solution (0.1 M, pH 7.2) at 25 °C.

Table 1 Association constants (K_S/M^{-1}), standard free energy ($\Delta G°$/kJ mol^{-1}), enthalpic ($\Delta H°$/kJ mol^{-1}), and entropic changes ($T\Delta S°$/kJ mol^{-1}) for 1 : 1 inclusion complexation in pH 7.2 phosphate buffer at 25 °C

Guest	Host	K_S	$\Delta G°$	$\Delta H°$	$T\Delta S°$
CA	β-CD[a]	$(4.07 \pm 0.08) \times 10^3$	−20.6	−23.0 ± 0.5	−2.4
	1[b]	$(1.40 \pm 0.01) \times 10^4$	−23.64 ± 0.01	−22.33 ± 0.82	1.41 ± 0.81
	2[b]	$(3.70 \pm 0.02) \times 10^3$	−20.35 ± 0.02	−38.46 ± 2.31	−17.99 ± 2.32
DCA	β-CD[a]	$(4.84 \pm 0.02) \times 10^3$	−21.0	−25.8 ± 0.0	−4.8
	1[b]	$(1.34 \pm 0.02) \times 10^4$	−23.53 ± 0.04	−52.75 ± 0.55	−29.09 ± 0.57
	2[b]	$(4.57 \pm 0.15) \times 10^3$	−20.87 ± 0.08	−68.29 ± 4.33	−47.29 ± 4.41
GCA	β-CD[a]	$(2.35 \pm 0.07) \times 10^3$	−19.3	−23.0 ± 0.1	−3.7
	1[b]	$(8.89 \pm 0.16) \times 10^3$	−22.55 ± 0.04	−42.07 ± 0.35	−19.53 ± 0.39
	2[b]	$(4.56 \pm 0.16) \times 10^3$	−20.87 ± 0.08	−37.64 ± 2.26	−16.65 ± 2.38
TCA	β-CD[a]	$(2.29 \pm 0.01) \times 10^3$	−19.2	−23.8 ± 0.1	−4.6
	1[b]	$(7.82 \pm 0.07) \times 10^3$	−22.20 ± 0.02	−45.84 ± 0.19	−23.52 ± 0.20
	2[b]	$(6.98 \pm 0.11) \times 10^3$	−21.92 ± 0.04	−45.59 ± 0.86	−23.56 ± 0.91

[a] Ref. 15. [b] This work.

between host **2** and guests. These results further demonstrate that CB[7] can profoundly alter the charge distribution and geometric configuration in the host–guest complexes, which is further validated from the viewpoint of the thermodynamic origins in the enthalpic and entropic changes as discussed below.

It is well-documented that the positive contribution to enthalpic changes ($\Delta H° < 0$) mainly originates from the hydrogen-bonding network, π-stacking arrangement, and ion–dipole interaction, while the electrostatic contact, conformational freedom, and solvent reorganization always lead to a favorable entropic change ($T\Delta S° > 0$).[16] Thermodynamically, the binding process of **1** and **2** with four steroid derivatives is mostly controlled by the favorable enthalpic gain and unfavorable entropic loss, except for CA⊂**1** with a slight entropic gain. This thermodynamic result of CA⊂**1** is mainly contributed to by the strong ion–ion attraction between the carboxylic tail of CA and the positively charged terminal sites of bispyridinium spacers on **1**, as well as the remarkable reorganization process of solvent molecules, which jointly overwhelm the entropic loss in the geometrical fixation upon host–guest complexation. Conversely, the ion–dipole and hydrogen-bonding interactions with the carbonyl groups around the two portals of CB[7] can facilitate the dispersion of positive charges on the bispyridinium plane.[17] These structural characteristics in CA⊂**2** and DCA⊂**2**, as compared to the ones in CA⊂**1** and DCA⊂**1**, can seriously weaken the electrostatic contact between the oppositely charged carboxylic acid anions and quaternary ammonium cations, leading to the large entropic loss in CA⊂**2** and DCA⊂**2**. In contrast, due to the mismatching of ionic

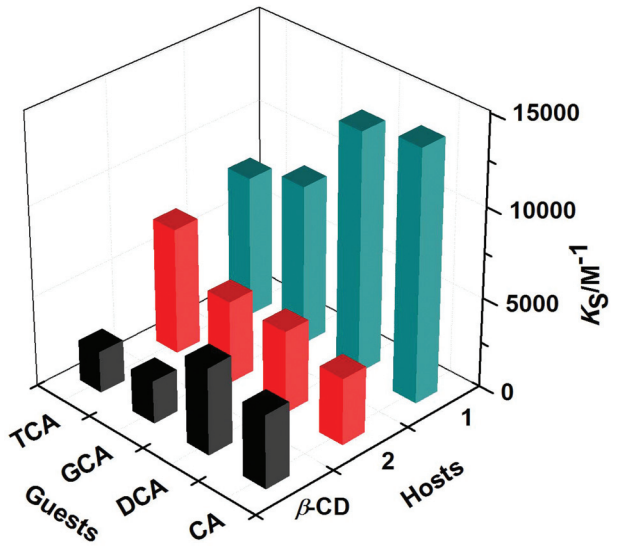

Fig. 8 Three-dimensional bars of K_S values in the investigated host–guest complexes.

distance between the bispyridinium center and the hydrophilic tail, the electrostatic interaction is comparable in the complexation of hosts **1** and **2** with GCA and TCA, and therefore, gives a rather similar entropic change.

Apart from the van der Waals forces upon host–guest complexation, the intrinsic hydrogen bonding interconnection can also play an indispensable role for the large negative enthalpic changes in aqueous solution. As compared to host **1**, the carbonyl groups of CB[7] in **2** can provide extra hydrogen bonding sites to give more favorable enthalpic gains upon complexation with CA and DCA. However, the large entropic loss in the presence of CB[7] can seriously decrease the superiority in these enthalpic gains, and therefore, the ΔG° values in CA⊂**1** and DCA⊂**1** are much lower than the ones in CA⊂**2** and DCA⊂**2**. Comparatively, this regularity in the enthalpic changes is distinctly changed in the case of **1** and **2** with GCA, probably because CB[7] as a severe steric hindrance may greatly deter the carboxylic tail of GCA from effective C–H···O hydrogen bonding interaction with the bispyridinium backbone in **2**. Moreover, along with the entropic changes in TCA⊂**1** and TCA⊂**2**, CB[7] cannot exert any tremendous influence on the existing binding mode between **1** and TCA, thus leading to very similar enthalpic changes.

In comparison to other guests, it is noteworthy that the complexation of **1** and **2** with DCA always gives the largest enthalpic and entropic changes. This phenomenon may be attributed to the more hydrophobic property of the DCA skeleton. This means, that because it lacks a hydroxyl group at C-7 position, DCA can be readily encapsulated in the CD cavity, and consequently, induce a more favorable hydrophobic interaction with the host compounds, which is responsible for the large enthalpic gain upon complexation. Meanwhile, the strongly associated complex may cause the high degree of order in the molecular binding system, thus accompanied by the obvious entropic loss in DCA⊂**1** and DCA⊂**2**. Therefore, combining these ITC data with the aforementioned 2D NMR results, it can be rationalized that the thermodynamic origins and binding modes could be precisely manipulated by the complexation of bispyridinium salt with CB[7] in aqueous solution.

Conclusion

In conclusion, the bispyridinium-tethered bis(β-CD) (**1**) and its CB[7]-mediated [2]rotaxane (**2**) are newly synthesized, exhibiting quite different molecular binding behaviors with bile salts in water. Although the corresponding [2]rotaxane cannot profoundly enhance the binding affinity toward steroid substrates, the presence of the CB[7] macrocycle can dramatically influence the electrostatic attraction and hydrogen-bonding interconnection in the resultant complexes. The intensive positive charges on the bispyridinium axle of **1** can facilitate close communication in the supramolecular complexes, whereas the diffusion of positive charges through CB[7] is unfavorable to form a tightly compact electrostatic complex, and then induce a significant change in the enthalpic and entropic distribution of thermodynamic origins. Superior to the linear receptors, we also envision herein that the wheel components in rotaxane structures may act as a demanding regulator to control the thermodynamic properties in many other supramolecular systems.

Experimental section

General method

All chemical reagents were commercially available unless noted otherwise. NMR data were recorded on 300 or 400 MHz spectrometer. All chemical shifts were referenced to the internal acetonitrile signal at 2.06 ppm.[18] The cyclic voltammetry measurements were carried out at 25 °C on an electrochemical analyzer. The working electrode was glassy carbon, the counter electrode was Pt coil, and the reference electrode was Ag/AgCl electrode, respectively. Mass spectra were performed on an ESI mode MS.

A thermostated and fully computer-operated isothermal calorimetry instrument was used for all the microcalorimetric experiments. The ITC experiments were performed at 25 °C in aqueous buffer solution, giving the stability constants (K_S) and the thermodynamic parameters upon complexation. In each run, a solution of host in a 0.250 mL syringe was sequentially injected with stirring at 300 rpm into a solution of guest in the sample cell (1.4227 mL volume). A control experiment to determine the heat of dilution was carried out for each run by performing the same number of injections with the same concentration of host compound as used in the titration experiments into the same solution without the guest compound. The dilution enthalpies determined in control experiments were subtracted from the enthalpies measured in the titration

experiments to obtain the net reaction heat. All thermodynamic parameters reported in this work were obtained by using the 'one set of binding sites' model. Two titration experiments were independently performed to give self-consistent parameters and the averaged values.

Synthesis of di(butynyl) bispyridinium salt (3)

A mixture of 4,4′-bipyridine (0.26 g, 1.67 mmol) and 4-bromo-1-butyne (625 μL, 6.7 mmol) in 10 mL of dry DMF was heated at 80 °C for 48 h. After cooling to room temperature, the precipitate produced was filtered and washed with dry DMF and CH_3CN to afford the product as a yellow solid in 94% yield. ^{1}H NMR (400 MHz, D_2O, ppm): δ 9.09 (d, J = 6.8 Hz, 4H), 8.47 (d, J = 6.7 Hz, 4H), 4.78 (t, J = 6.2 Hz, 4H), 2.93 (tt, J = 8.1, 4.0 Hz, 4H), 2.41 (t, J = 2.6 Hz, 2H). ^{13}C NMR (100 MHz, D_2O, ppm): δ 150.5, 145.8, 127.0, 78.4, 74.2, 59.9, 20.7. MALDI-MS: m/z calcd for $C_{18}H_{18}N_2$ $[M - 2Br]^{+\bullet}$: 262.1465, found: 262.1471.

Synthesis of bispyridinium-bridged bis(β-cyclodextrin) (1)

A solution of mono-6-deoxyl-6-azido-β-CD (1.5 g, 1.3 mmol) in 20 mL of water was added to a solution of compound **3** (131 mg, 0.3 mmol) and $CuSO_4{\cdot}5H_2O$ (500 mg, 2.0 mmol) in 10 mL of water. The mixture was heated at 80 °C for 10 min, and then sodium ascorbate (0.8 g, 4.0 mmol) in 10 mL of water was added. The resulting mixture was kept at 80 °C under an atmosphere of nitrogen for 24 h. After cooling to room temperature, insoluble precipitates were removed by filtration, and the reaction mixture was evaporated under reduced pressure to dryness. The residue was dissolved in a small amount of water, and washed with acetone at least three times. The crude product was subjected to a medium-pressure liquid chromatography (MPLC) system using a gradient elution system of distilled water and ethanol gradient with ethanol from 0 to 4% at a flow rate of 5 mL min^{-1}. The detector wavelength was set at 264 nm. After drying under vacuum, the target compound was obtained as a brown solid in 43% yield. ^{1}H NMR (400 MHz, D_2O, ppm): δ 8.94 (s, 4H), 8.42 (s, 4H), 7.86 (s, 2H), 4.86–4.96 (m, 18H), 3.33–4.08 (m, 88H), 3.06–3.09 (m, 2H), 2.76–2.79 (m, 2H); ^{13}C NMR (100 MHz, D_2O, ppm): δ 150.2, 145.6, 141.9, 127.0, 126.1, 102.0, 101.8, 101.5, 83.0, 81.3, 81.1, 80.9, 73.0, 72.8, 72.6, 72.0, 71.9, 71.8, 71.7, 71.4, 70.4, 61.0, 60.4, 60.3, 59.2, 51.1, 26.5. MALDI-MS: m/z calcd for $C_{102}H_{156}N_8O_{68}$ $[M - 2Br]^{+\bullet}$: 2580.8984, found: 2580.8999.

Synthesis of [2]rotaxane (2) containing bispyridinium salt as axle and cyclodextrins as stopper

A solution of compound **3** (133 mg, 0.3 mmol) and CB[7] (592 mg, 0.5 mmol) in 30 mL of water was stirred at room temperature for 0.5 h. Then, mono-6-deoxyl-6-azido-β-CD (1.5 g, 1.3 mmol), $CuSO_4{\cdot}5H_2O$ (500 mg, 2.0 mmol), and sodium ascorbate (0.8 g, 4.0 mmol) were added to the resulting solution. The reaction mixture was heated at 50 °C under an atmosphere of nitrogen for 24 h. Compound **2** was purified by the same procedure as described above to afford yellow solid in 27% yield. ^{1}H NMR (400 MHz, D_2O, ppm): δ 8.97 (d, 4H), 8.07 (s, 2H), 6.92 (d, 4H), 5.55 (d, 14H), 5.42 (s, 14H), 4.91–5.16 (m, 18H), 4.06 (d, 14H), 3.34–4.07 (m, 88H), 3.20 (d, 2H), 2.65 (d, 2H); ^{13}C NMR (100 MHz, D_2O, ppm): δ 156.1, 149.2, 147.8, 142.1, 126.2, 122.8, 102.2, 101.9, 101.8, 101.7, 83.4, 81.1, 81.0, 73.0, 72.9, 72.7, 72.1, 72.0, 71.8, 71.4, 71.2, 70.8, 69.9, 61.1, 60.2, 59.2, 52.7, 51.4, 26.3. MALDI-MS: m/z calcd for $C_{144}H_{198}N_{36}O_{82}$ $[M - 2Br]^{+\bullet}$: 3743.2430, found: 3743.2450.

Acknowledgements

This work was financially supported by 973 Program (2011CB932502), NNSFC (no. 20932004, 91227107, and 21102075).

References

1 (*a*) M. E. Brewster and T. Loftsson, *Adv. Drug Delivery Rev.*, 2007, **59**, 645–666; (*b*) M. Kralj, L. Tušek-Božić and L. Frkanec, *ChemMedChem*, 2008, **3**, 1478–1492; (*c*) S. Walker, R. Oun, F. J. McInnes and N. J. Wheate, *Isr. J. Chem.*, 2011, **51**, 616–624; (*d*) Á. Martínez, C. Ortiz Mellet and J. M. García Fernández, *Chem. Soc. Rev.*, 2013, **42**, 4746–4773; (*e*) S. B. Nimsea and T. Kim, *Chem. Soc. Rev.*, 2013, **42**, 366–386.

2 (*a*) S. A. Nepogodiev and J. F. Stoddart, *Chem. Rev.*, 1998, **98**, 1959–1976; (*b*) L. X. Song, L. Bai, X. M. Xu, J. He and S. Z. Pan, *Coord. Chem. Rev.*, 2009, **253**, 1276–1284; (*c*) A. Harada, A. Hashidzume, H. Yamaguchi and Y. Takashima, *Chem. Rev.*, 2009, **109**, 5974–6023; (*d*) X. Ma and H. Tian, *Chem. Soc. Rev.*, 2010, **39**, 70–80.

3 (*a*) K. Uekama, F. Hirayama and T. Irie, *Chem. Rev.*, 1998, **98**, 2045–2076; (*b*) F. van de Manakker, T. Vermonden, C. F. van Nostrum and W. E. Hennink, *Biomacromolecules*, 2009, **12**, 3157–3175; (*c*) Y. Chen and Y. Liu, *Chem. Soc. Rev.*, 2010, **39**, 495–505; (*d*) J. J. Li, F. Zhao and J. Li, *Appl. Microbiol. Biotechnol.*, 2011, **90**, 427–443; (*e*) H. D. Williams, N. L. Trevaskis, S. A. Charman, R. M. Shanker, W. N. Charman, C. W. Pouton and C. J. H. Porter, *Pharmacol. Rev.*, 2013, **65**, 315–499.

4 (*a*) R. F. Gómez-Biagi, R. B. C. Jagt and M. Nitz, *Org. Biomol. Chem.*, 2008, **6**, 4622–4626; (*b*) L. Wang, C. Zhong, P. Xue and E. Fu, *J. Org. Chem.*, 2011, **76**, 4874–4883; (*c*) J. M. Casas-Solvas, I. Quesada-Soriano, D. Carreño-Gázquez, J. J. Giménez-Martínez, L. García-Fuentes and A. Vargas-Berenguel, *Langmuir*, 2011, **27**, 9729–9737.

5 (*a*) J. M. Adam, D. J. Bennett, A. Bom, J. K. Clark, H. Feilden, E. J. Hutchinson, R. Palin, A. Prosser, D. C. Rees, G. M. Rosair, D. Stevenson, G. J. Tarver and M.-Q. Zhang, *J. Med. Chem.*, 2002, **45**, 1806–1816; (*b*) A. Bom, M. Bradley, K. Cameron, J. K. Clark, J. van Egmond, H. Feilden, E. J. MacLean, A. W. Muir, R. Palin, D. C. Rees and M.-Q. Zhang, *Angew. Chem., Int. Ed.*, 2002, **41**, 265–270.

6 (*a*) H. Wang, R. Cao, C.-F. Ke, Y. Liu, T. Wada and Y. Inoue, *J. Org. Chem.*, 2005, **70**, 8703–8711; (*b*) Y. Chen, F. Li, B.-W. Liu, B.-P. Jiang, H.-Y. Zhang, L.-H. Wang and Y. Liu, *J. Phys. Chem. B*, 2010, **114**, 16147–16155.

7 (*a*) C. F. J. Faul and M. Antonietti, *Adv. Mater.*, 2003, **15**, 673–683; (*b*) K. Binnemans, *Chem. Rev.*, 2005, **105**, 4148–4204; (*c*) B. Rybtchinski, *ACS Nano*, 2011, **5**, 6791–6818.

8 (*a*) M. V. Rekharsky and Y. Inoue, *Chem. Rev.*, 1998, **98**, 1875–1917; (*b*) L. Lei and Q.-X. Guo, *J. Inclusion Phenom. Macrocyclic Chem.*, 2002, **42**, 1–14; (*c*) H.-J. Schneider, *Angew. Chem., Int. Ed.*, 2009, **48**, 3924–3977; (*d*) R. N. Dsouza, U. Pischel and W. M. Nau, *Chem. Rev.*, 2011, **111**, 7941–7980; (*e*) M. Xue, Y. Yang, X. Chi, Z. Zhang and F. Huang, *Acc. Chem. Res.*, 2012, **45**, 1294–1308.

9 (*a*) Y. Liu, Y. Song, H. Wang, H.-Y. Zhang and X.-Q. Li, *Macromolecules*, 2004, **37**, 6370–6375; (*b*) K. Sakamoto, Y. Takashima, N. Hamada, H. Ichida, H. Yamaguchi, H. Yamamoto and A. Harada, *Org. Lett.*, 2011, **13**, 672–675.

10 C. Hocquelet, J. Blu, C. K. Jankowski, S. Arseneau, D. Buisson and L. Mauclaire, *Tetrahedron*, 2006, **62**, 11963–11971.

11 (*a*) I. W. Wyman and D. H. Macartney, *Org. Biomol. Chem.*, 2010, **8**, 253–260; (*b*) M. J. Pisani, Y. Zhao, L. Wallace, C. E. Woodward, F. R. Keene, A. I. Day and J. G. Collins, *Dalton Trans.*, 2010, **39**, 2078–2086; (*c*) H. Cong, C.-R. Li, S.-F. Xue, Z. Tao, Q.-J. Zhu and G. Wei, *Org. Biomol. Chem.*, 2011, **9**, 1041–1046; (*d*) A. Thangavel, C. Sotiriou-Leventis, R. Dawes and N. Leventis, *J. Org. Chem.*, 2012, **77**, 2263–2271.

12 Y.-L. Zhao, D. Benítez, I. Yoon and J. F. Stoddart, *Chem.–Asian J.*, 2009, **4**, 446–456.

13 D. Neuhaus and M. Williamson, *The Nuclear Overhauser Effect in Structural and Conformational Analysis*, VCH Publishers, New York, 1989.

14 (*a*) Y. Liu, C.-F. Ke, H.-Y. Zhang, J. Cui and F. Ding, *J. Am. Chem. Soc.*, 2008, **130**, 600–605; (*b*) K. Yamauchi, A. Miyawaki, Y. Takashima, H. Yamaguchi and A. Harada, *Org. Lett.*, 2010, **12**, 1284–1286; (*c*) S. Menuel, N. Azaroual, D. Landy, N. Six, F. Hapiot and E. Monflier, *Chem.–Eur. J.*, 2011, **17**, 3949–3955; (*d*) J. Potier, S. Menuel, N. Azaroual, E. Monflier and F. Hapiot, *Eur. J. Org. Chem.*, 2014, 1547–1556.

15 Y. Liu, Y.-W. Yang, R. Cao, S.-H. Song, H.-Y. Zhang and L.-H. Wang, *J. Phys. Chem. B*, 2003, **107**, 14130–14139.

16 (*a*) C. Bonal, Y. Israëli, J.-P. Morel and N. Morel-Desrosiers, *J. Chem. Soc., Perkin Trans. 2*, 2001, 1075–1078; (*b*) Y. Liu, D.-S. Guo, H.-Y. Zhang, Y.-H. Ma and E.-C. Yang, *J. Phys. Chem. B*, 2006, **110**, 3428–3434; (*c*) L. Chen, Y.-M. Zhang and Y. Liu, *J. Phys. Chem. B*, 2012, **116**, 9500–9506.

17 (*a*) H.-J. Kim, W. S. Jeon, Y. H. Ko and K. Kim, *Proc. Natl. Acad. Sci. U. S. A.*, 2002, **99**, 5007–5011; (*b*) Y. Ling, J. T. Mague and A. E. Kaifer, *Chem.–Eur. J.*, 2007, **13**, 7908–7914; (*c*) V. Kolman, M. Babinský, P. Kulhánek, R. Marek and V. Sindelar, *New J. Chem.*, 2011, **35**, 2854–2859; (*d*) N. S. Venkataramanan, S. Ambigapathy, H. Mizuseki and Y. Kawazoe, *J. Phys. Chem. B*, 2012, **116**, 14029–14039.

18 H. E. Gottlieb, V. Kotlyar and A. Nudelman, *J. Org. Chem.*, 1997, **62**, 7512–7515.